CAFE simulation of columnar-to-equiaxed transition in Al-7wt%Si alloys directionally solidified under microgravity

CAFE simulation of columnar-to-equiaxed transition in Al-7wt%Si alloys directionally solidified under microgravity

D R Liu[1a], N Mangelinck-Noël[2,3], Ch-A Gandin[4], G Zimmermann[5], L Sturz[5], H Nguyen Thi[2,3] and B Billia[2,3]

[1] School of Materials Science and Engineering, Harbin University of Science and Technology, No. 4 Lin Yuan Road, Xiang Fang District, Harbin 150040, China
[2] Aix-Marseille University and [3] CNRS, IM2NP, UMR CNRS 7334, campus Saint-Jérôme, Case 142, 13397 Marseille Cedex 20, France
[4] MINES ParisTech, CEMEF, CNRS UMR 7635, Sophia Antipolis, France
[5] ACCESS e.V., Aachen, Germany

E-mail: [a] nacylake@126.com

Abstract. A two-dimensional multi-scale cellular automaton - finite element (CAFE) model is used to simulate grain structure evolution and microsegregation formation during solidification of refined Al-7wt%Si alloys under microgravity. The CAFE simulations are first qualitatively compared with the benchmark experimental data under microgravity. Qualitative agreement is obtained for the position of columnar to equiaxed transition (CET) and the CET transition mode (sharp or progressive). Further comparisons of the distributions of grain elongation factor and equivalent diameter are conducted and reveal a fair quantitative agreement.

1. Introduction

Grain morphology has a great influence on the final performance of as-cast products [1]. Depending on the applied processing parameters and the alloy physical properties, solidified grain structures could be purely columnar, or totally equiaxed, or a mixture of columnar and equiaxed. Columnar grains often grow from near the mold surface under a highly imposed thermal gradient [2]. Although, the castings with columnar structure significantly increase the strength in the columnar direction, columnar structures have been found to be more prone to cracking. Castings of equiaxed structure are desirable for many applications, since they exhibit homogeneity in physical and mechanical properties [3]. Therefore, an accurate control of columnar-to-equiaxed transition (CET) and a quantitative understanding of the relationship between CET and casting parameters are essential to industrial application and scientific development.

Within the ESA CETSOL (Columnar to Equiaxed Transition in SOLidification Processing) project, six experiments with different solidification parameters were carried out to study CET transition under microgravity in the Microgravity Science Laboratory (MSL), using the Low Gradient Furnace (LGF) on board the International Space Station (ISS) [4]. Experimental characterizations of the experimental samples were performed by Zimmermann et al. [4], Mirihanage et al. [5] and Liu et al. [6]. Experimental studies are essential to identify mechanisms at the state of CET. However, during solidification, a complex interplay of multi-scale phenomena cannot be observed and then, numerical modelling offers the possibility to study the CET mechanism and the parameter impacts in details.

Direct macroscopic modelling, such as cellular automaton - finite element (CAFE) model, has been developed by Gandin and co-workers with advantages in numerically investigating CET [7,8]: at the size of casting, the topological description of grain structure transition and composition heterogeneity can be realized. Comparisons with benchmark experimental data obtained from microgravity experiments are necessary to guide further improvement of model.

In this publication, CAFE simulations of CET transition during solidification of refined Al-7wt%Si alloys under microgravity are compared with benchmark experimental data. Three aspects are considered: distributions of grain equivalent diameter and elongation factor, CET position and CET transition mode. The influence of pulling-velocity jump on CET is investigated. The reason why simulations cannot quantitatively match some of the experimental results is discussed.

2. Experiment

The schematic setup of the sample cartridge assembly inserted in the low gradient furnace (LGF) available in the Materials Science Laboratory (MSL) on board the International Space Station (ISS) was presented in [4-6]. Rod-like samples of 7.8 mm in diameter and 245 mm in length were placed in a protective Al_2O_3 cylindrical crucible. The main solidification parameters are summarized in table 1[4]. In the present article, we focus on the samples (FM1 / FM5) which are refined Al-7wt%Si alloys with 0.5 wt % Al – 5 wt% Ti – 1 wt% B refiner. Processing conditions are identical except the pulling velocity. In FM1, a pulling-velocity jump is applied from 0.01 mm s^{-1} in stage I to 0.2 mm s^{-1} in stage II. For FM5, the pulling velocity keeps at a low constant value, 0.01 mm s^{-1}, through stages I and II.

Table 1. Processing parameters for samples solidified under microgravity, where V_n is the furnace pulling velocity and S_n the solidification length under V_n.

Sample (µg)	FM1	FM5
Grain refined	Yes	Yes
Homogenization time (s)	600	600
Initial gradient (^{o}C mm^{-1})	0.9	0.9
Stage I		
Time interval (s)	0 ~ 2000	0 ~ 2000
V_1 (mm s^{-1})	0.01	0.01
S_1 (mm)	20	20
Stage II		
Time interval (s)	2000 ~ 2250	2000 ~ 4000
V_2 (mm s^{-1})	**0.2**	**0.01**
S_2 (mm)	50	20
Cooling rate (^{o}C s^{-1})	0.067	0.067
Stage III		
V_3 (mm s^{-1})	3	3

The characterization of the experimental grain structure was performed using electron backscattered diffraction (EBSD). For each identified grain, the grain equivalent diameter and grain elongation factor were calculated based on the numerical analyses of EBSD output data file. The equivalent diameter of a non-spherical object is equal to the diameter of a sphere of equivalent area [6]. The elongation factor is defined as the major axis length to the minor axis length ratio. The two axes intersect orthogonally at the centroid of the grain [6].

The end of columnar growth is determined by visual examination of the polished sample surface. On the one hand, the highest position of dendrites which develop from the beginning of solidification is named as CET_{min}, that is the top boundary of columnar zone. On the other hand, the definition of CET position between transition zone and equiaxed region is dependent on the distribution pattern of averaged elongation factor along the solidification direction. A critical elongation factor equal to 2 [9] is chosen as a criterion. If the profile of the averaged elongation factor varies around 2 within an area, an intermediate zone exists where equiaxed and short elongated grains coexist. If the profile drops below 2 at a position and barely bounces back, an equiaxed region is established and this position is defined as CET_{max}. If there is only CET_{min} identified, a sharp CET from columnar to equiaxed grains occurs. If CET_{min} and CET_{max} coexist, an intermediate region forms and the CET mode is progressive.

The difference in CET transition manner between FM1 and FM5 is explained as: a pulling-velocity jump used in FM1 leads to a higher degree of constitutional undercooling ahead of the solidification front. Under such condition, the nucleation rate is enhanced. With an intensive and frequent nucleation of grains in the liquid, the newly nucleated grains compete over the continued growth of existing grains to form a truly equiaxed zone after columnar zone [9].

3. Modelling

3.1. CAFE modelling
Conservation equations over finite element mesh (FE) are solved using a volume averaging approach. A more detailed presentation of these equations is presented elsewhere [7,8]. For simulation of solidification under microgravity, the computation of momentum equation is switched off. A few assumptions are made. (i) Equal and constant densities in the phases. (ii) No movement of solid phase. (iii) Only heterogeneous nucleation of equiaxed grains is considered.

The FE mesh is divided into a regular lattice of fine square named CA cells. The CA technique is used to track the development of grain envelopes. A Gaussian distribution is adopted to describe nucleation of equiaxed grains [8]. Three input parameters are needed: mean nucleation undercooling ΔT_{mean}, the standard deviation ΔT_{σ} and maximum nucleation density N_{max}. A dendrite tip kinetics defined in [8] is used to calculate dendrite growth.

3.2. Calculation domain, boundary and initial conditions
The experimental system that includes the sample cartridge assembly and the heating system is not directly simulated. The right half of cylindrical geometries, including alloy sample, crucible and plug, are chosen as the computational domains (figure 1). The configuration is two-dimensional and axi-symmetrical. Since the bottom part of the sample ranging from 0 mm to 70 mm remains at solid state through the whole experimental process, the alloy sample is numerically divided into two parts. The top part is simulated using CAFE model and the bottom using only FE model.

To simulate the directional solidification, Dirichlet thermal boundary conditions [10] are used in this study by imposing temperature profiles on the outer surface of three sub-domains "plug", "top crucible" and "bottom crucible".

Twelve input cooling curves (TC1 to TC12) are placed on the outer surface of the top crucible (figure 1) and correspond to experimentally measured profiles. The thermocouple positions range from (TC1) 72.5 mm to (TC12) 182.5 mm defined from the reference plane (0 mm). Another five temperature profiles (SC0: -5.0 mm, SC13: 202.5 mm, SC14: 222.5 mm, SC15: 243.0 mm and SC16: 281.5 mm) are imposed to strictly maintain the unidirectional heat flow through the "Al7Si alloy" domain. These temperature profiles are defined as a function of time by propagating the time evolution of the temperature gradients between thermocouples TC1 and TC2, TC11 and TC12, TC12 and SC13, SC13 and SC14, SC14 and SC15.

At the beginning of the simulation, the whole system has an initial temperature of 800.0 $^{\circ}$C. Five nuclei with different growth orientations and with a nucleation undercooling of 0 $^{\circ}$C are fixed at the bottom boundary of "Al7Si alloy" domain to reproduce the columnar grain nucleation and competition.
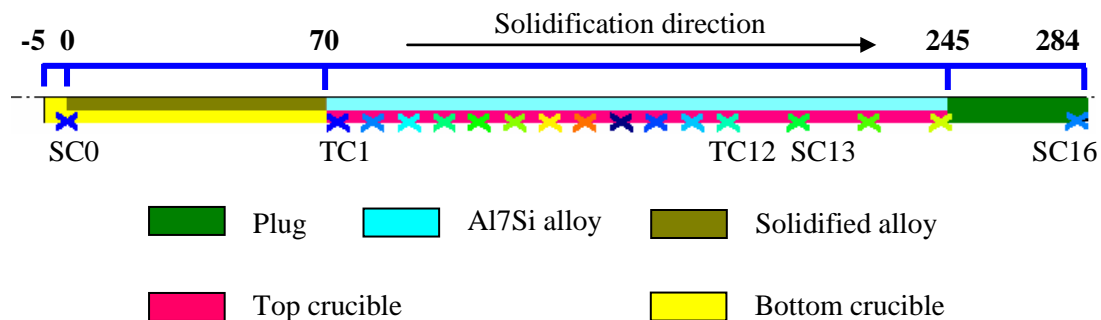
Figure 1. Schematic drawing of casting system with two-dimensional axi-symmetrical coordinates. All dimensions are in mm.

CAFE model is used through the software XR2Sol-CAFE developed by MINES ParisTech CEMEF. The thermo-physical properties of Al-7wt% Si alloy are presented in details in [11]. Here, only critical parameters used in the present CAFE simulations are listed. FE mesh size is 0.3 mm and CA cell size 0.04 mm. The heat transfer coefficients at alloy / crucible, alloy / plug and crucible / plug interfaces are 10^4 W m^{-2} ^{o}C^{-1}, 10^3 W m^{-2} ^{o}C^{-1} and 10^3 W m^{-2} ^{o}C^{-1}, respectively. The nucleation parameters ΔT_{mean} = 4 ^{o}C, ΔT_σ = 0.5 ^{o}C and N_{max} = 5×10^{10} m^{-3} are chosen to get a match with the experimentally observed grain structures in FM1. All these parameters stay the same for different simulation cases. These parameters are kept constant for all the simulations.

4. Results and discussion

4.1. CAFE simulation of grain structure
Figure 2 compares the distributions of averaged grain elongation factor and equivalent diameter along two sections (L4 and L5) cut in the longitudinal direction obtained from EBSD analyses (dashed line) and from CAFE simulations (solid line) [12]. The experimental CET values given here agree with the values obtained from grain size analysis in [13]. According to the definition methodology proposed in section 2, for FM1, the predicted CET_{min} is 130 mm very close to the measured 127 mm (figure 2(a)). For FM5, both simulation and experiment show two CET positions (figure 2(a)). The simulated CET_{min} is 140 mm that is 10 mm higher than the measured 130 mm. The predicted CET_{max} is 165 mm which is 9 mm higher than the measured 156 mm.

A good agreement between simulation and experiment is obtained for the distribution of grain equivalent diameter for FM1 (figure 2(b)). In simulations, 67 % and 78 % grains with a diameter smaller than 1.0 mm on sections L4 and L5 are measured, respectively, which is close to the respective experimental measurements of 65 % and 63%. For FM5 (figure 2(b)), the general tendency that grain size decreases from the intermediate zone to the equiaxed zone is reproduced. Without the application of the pulling-velocity jump, both simulation and experiment present a coarse and non-homogenous grain structure. In simulations, 19% and 31 % grains with a diameter smaller than 1.0 mm on sections L4 and L5 are measured respectively, which are different from the respective experimental measurements of 43% and 53 %. Difference between simulations and experiments is attributed to the fact that the formation and development of the grain structure in the two-dimensional axi-symmetrical simulation do not exactly correspond to the real experiments regarding the number of effective nuclei, the random growing orientations, and the branching in 3D. This discrepancy is less pronounced for the cases where many grains are formed, because statistical reasons minor these effects.
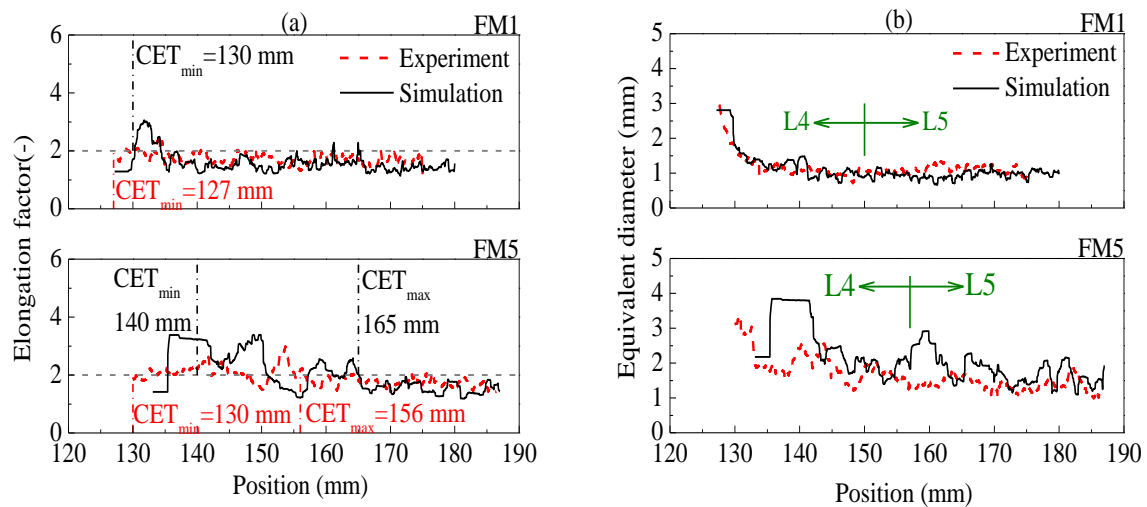
Figure 2. Comparison of (a) grain elongation factor and (b) grain equivalent diameter simulated using CAFE model in black with experimental measurements in red on sections L4 and L5: FM1 (refined Al - 7 wt% Si alloy, $V_2 = 0.2$ mm s^{-1}); FM5 (refined Al - 7 wt% Si alloy, $V_2 = 0.01$ mm s^{-1}). Superimposed red and black vertical dash-dotted lines in (a) correspond to experimentally-measured and predicted CET positions, respectively.
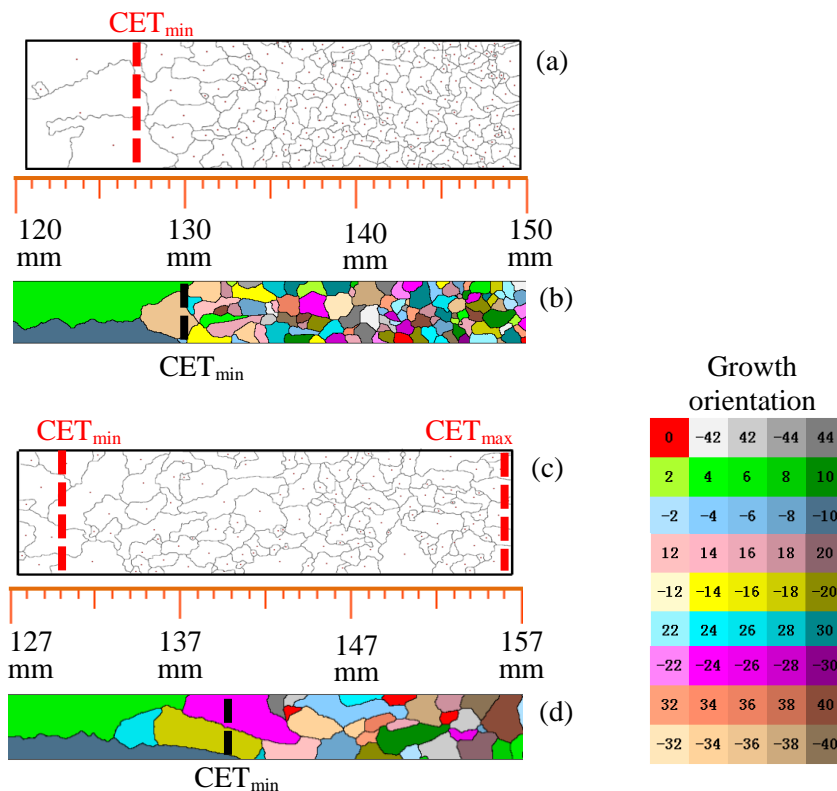

Figure 3. Comparisons of grain structures on section L4 (b) and (d) simulated using CAFE model with (a) and (c) EBSD measurements. (a) and (b) FM1 (refined Al - 7 wt% Si alloy, $V_2 = 0.2$ mm s^{-1}); (c) and (d) FM5 (refined Al - 7 wt% Si alloy, $V_2 = 0.01$ mm s^{-1}).

Figure 3 compares grain structures on section L4 obtained from EBSD analyses (figures 3(a) and (c)) and from CAFE simulations (figures 3(b) and (d)) [12]. From the simulated grain structures, it can be noted that the CET is sharp for FM1 (figure 3(b)) since there is only one CET position (CET_{min}). For FM5 (figure 3(d)), the CET is progressive. The two CET positions (CET_{min} and CET_{max}) are located on sections L4 and L5, respectively. The predicted CET transition mode is consistent with experimental observations.

5. Conclusion

Numerical simulations of two MSL-LGF microgravity experiments (FM1 and FM5) performed using CAFE model are compared qualitatively and quantitatively with the experiments. The influence of the pulling velocity on the grain structure is qualitatively and quantitatively reflected in CAFE simulations. The CET transition mode, be it sharp or progressive, is retrieved. Distributions of grain elongation factor and equivalent diameter are fairly reproduced. The discrepancy between the predicted and measured CET positions is due to the fact that the grain structure development in the two-dimensional axi-symmetrical simulations does not correspond to that in the experiments regarding the nucleation positions and growth orientations. The distributions of grain size and elongation factor are retrieved but cannot be perfectly identical with experimental measurements due to the statistical aspect of nucleation events.

References

[1]   Spittle JA 2006 *Int. Mater. Rev.* **51** 247
[2]   Chen Y, Bogno AA, Xiao NM, Billia B, Kang XH, Nguyen-Thi H, Luo XH, Li DZ 2012 *Acta Mater.* **60** 199
[3]   Reinhart G, Gandin Ch-A, Mangelinck-Noël N, Nguyen-Thi H, Spinelli JE, Baruchel J, Billia B 2013 *Acta Mater.* **61** 4765
[4]   Zimmermann G, Sturz L, Billia B, Mangelinck-Noël N, Nguyen-Thi H, Gandin Ch-A 2011 *J. Phys. Conferences Series* **327** 012003
[5]   Mirihanage WU, Browne DJ, Zimmermann G, Sturz L 2012 *Acta Mater.* **60** 6362
[6]   Liu DR, Mangelinck-Noël N, Gandin Ch-A, Zimmermann G, Sturz L, Nguyen-Thi H, Billia B 2014 *Acta Mater.* **64** 253
[7]   Gandin Ch-A 2010 *C. R. Phys.* **11** 216
[8]   Guillemot G, Gandin Ch-A, Bellet M 2007 *J. Cryst. Growth* **303** 58
[9]   Hunt JD 1984 *Mater. Sci. Eng.* **65** 75
[10]   Cruz K SD, Mangelinck-Noël N, Gandin Ch-A, Billia B 2011 *IOP Conf. Ser. Mater. Sci. Eng.* **27** 012017
[11]   Gandin Ch-A 2000 *ISIJ Int.* **40** 971
[12]   Liu DR, Mangelinck-Noël N, Gandin Ch-A, Zimmermann G, Sturz L, Nguyen-Thi H, Billia B 2015 *Acta Mater.* **In press**
[13]   Zimmermann G, Sturz L, Billia B, Mangelinck-Noël N, Liu DR, Nguyen-Thi H, Bergeon N, Gandin Ch-A, Browne DJ, Beckermann Ch, Tourret D, Karma A 2014 *Materials Science Forum* **790-791** 12